

A molecular mechanics approach to mapping the conformational space of diaryl and triarylphosphines†

Natalie Fey,^a James A. S. Howell,^{*b} Jonathan D. Lovatt,^b Paul C. Yates,^b Desmond Cunningham,^c Patrick McArdle,^c Hugo E. Gottlieb^d and Simon J. Coles^e

Received 14th July 2006, Accepted 28th September 2006

First published as an Advance Article on the web 13th October 2006

DOI: 10.1039/b610123b

A molecular mechanics force field has been developed which accurately reproduces experimental solid state structures and conformer interconversion barriers for a series of sterically congested diaryl and triaryl phosphines and some of their chalcogenide and Cr(CO)₅ derivatives.

Introduction

Phosphines and phosphites are ubiquitous ligands in the homogeneous catalysis of organic reactions using transition metal complexes, primarily because structural variation allows not only a fine tuning of activity and selectivity (including enantioselectivity)^{1a-g} but also because it can be used to alter catalyst properties such that they may be used in water,^{2a-d} fluorosolvents,^{3a,b} ionic liquids^{4a-c} or supercritical CO₂^{5a,b} or bound to solid supports.^{6a-c} Prominent among these ligands are triarylphosphines and chelating diphosphines terminated by a diarylphosphine motif. Chelating phosphines can be particularly effective in promoting asymmetric synthesis, and the interaction of the substrate with the array of phenyl rings presented by the catalyst is an important if not determining factor in enantioselection.

Although thorough quantum mechanics‡ calculations of 'real', conformationally flexible metal–phosphine complexes are still not realistically possible in terms of computational time, many recent studies have used quantum mechanics/molecular mechanics (QM/MM) methods in which QM and MM are applied either sequentially⁷ or (more often) simultaneously.^{8a,b} The MM component has been applied using a variety of common MM force fields which have not been ideally parameterised to deal with arylphosphines, though a parameterisation for alkyl phosphines has recently been reported.⁹ Other recent approaches have identified various metal–ligand descriptors which may be used

to correlate the steric and electronic properties of phosphine ligands.^{10a-c}

We report here the testing of an adapted MM force field for triaryl and alkyldiaryl phosphines and their chalcogenide and Cr(CO)₅ derivatives which can be incorporated into standard computational packages as an aid in the design of phosphines and phosphine complexes for use in catalysed organic synthesis. The force field has been tested against experimental structural and dynamic data obtained by X-ray crystallography and variable temperature NMR spectroscopy for a series of sterically congested 2-RC₆H₄ substituted derivatives. As previous calculations^{11a,b} on PPh₃ and HCPPh₃ indicate an almost flat energy surface in the torsion angle range 20 to 50° (A–B–C_{ipso}–C_α; A = lone pair, B = P; A = H, B = C), we have chosen to use experimental data from more sterically congested *ortho*-substituted derivatives where conformational energy minima are more clearly defined and both conformational equilibrium constants and interconversion barriers are measurable by variable temperature NMR techniques.

Results and discussion

Force field parameterisation

Equilibrium values for bond lengths and angles involving the phosphorus atom were derived from a survey of 55 relevant crystal structures retrieved from the Cambridge Crystallographic Data Base.¹² A slight underestimation of ideal bond lengths and angles proved more effective than the use of excessive force constants in controlling the reproduction of observed geometries. The lone pair–phosphorus distance was derived from an electron deformation density refinement of bis(diphenylphosphino)butane.¹³ The corresponding force constant was chosen to reproduce this distance. Stretching force constants for XP–PX terms (X = O, S, Se) were derived by extrapolation from the existing C=O term, taking experimentally determined stretching force constants into account.¹⁴ Unique labelling as described by Brown *et al.*^{15a,b} was implemented for the Cr(CO)₅ complexes. Brown's parameters for Cr–C bonds were adjusted until good agreement with the structure of (2-MeC₆H₄)₃PCr(CO)₅¹⁶ was achieved. Any torsion terms involving the chromium atom in Cr(CO)₅ complexes have been set to zero.

Phenylphosphine and its oxide and sulfide were used for parameterisation of the XP–PX–C3–C3 term. Diphenylphosphine

^aSchool of Chemistry, Cantock's Close, Clifton, Bristol, UK BS8 1TS. E-mail: natalie.fey@bristol.ac.uk; Fax: +44 (0)117 9251295; Tel: +44 (0)117 9546398

^bSchool of Physical and Geographical Sciences, Lennard Jones Laboratories, Keele University, Keele, Staffordshire, UK ST5 5BG. E-mail: j.a.s.howell@keele.ac.uk; Fax: +44 (0)1782 712378; Tel: +44 (0)1782 583041

^cChemistry Department, National University of Ireland, Galway, University Road, Galway, Eire. E-mail: des.cunningham@nuigalway.ie; p.mcardle@ucg.ie; Fax: +353 91 525700; Tel: +353 91 492460

^dChemistry Department, Bar Ilan University, Ramat Gan, 52900, Israel. E-mail: gottlieb@mail.biu.ac.il; Fax: +972 3 5351250; Tel: +972 3 5318828

^eSchool of Chemistry, University of Southampton, Highfield, Southampton, UK SO17 1BJ. E-mail: sjc5@soton.ac.uk; Fax: +44 (0)23 80593781; Tel: +44 (0)23 80596722

† Electronic supplementary information (ESI) available: NMR spectral data; force field parameterisation; variable temperature NMR lineshape analysis. See DOI: 10.1039/b610123b

‡ QM here is taken to include density functional theory calculations.

and its oxide and sulfide were used for parameterisation of the C3–PX–C3–C3 term. The required torsion to one ring was driven whilst the corresponding torsion to the other ring was allowed to optimise. Methylphosphine and its oxide and sulfide were used for parameterisation of the H–C4–PX–XP term. Bu^tphosphine and its oxide and sulfide were used for parameterisation of the C4–C4–PX–XP term. Methylphenylphosphine and its oxide and sulfide were used for parameterisation of the C3–C3–PX–C4 term.

Torsional parameters were classified as either phosphorus dependent or independent. Independent parameters are unlikely to be influenced significantly by the phosphorus substituents and should be fully transferable between different substituents. In contrast, dependent torsional parameters are potentially influenced by the extent of π -conjugation and are thus not transferable between different phosphine derivatives. For triarylphosphines, the torsions XP–PX–C3–C3 and C3–PX–C3–C3 were regarded as phosphorus dependent. Additionally for diarylphosphines and the corresponding oxides and sulfides the C4–PX–C3–C3, H–C4–PX–XP and C4–C4–PX–XP parameters were regarded as phosphorus dependent. Since these terms are potentially interdependent, they were parameterised using a literature procedure.^{17a,b} Using model compounds, an *ab initio* Hartree–Fock (HF) rotational energy profile was generated, whilst the same profile was produced at the MM level with the torsional constant of interest set to zero. The torsional energy potential function was then fitted to the difference plot to determine the magnitude of the torsional parameters. The MM torsional potential function $E_t = 0.5 V_1 [1 + \cos(\phi)] + 0.5 V_2 [1 - \cos(2\phi)] + 0.5 V_3 [1 + \cos(3\phi)]$ was fitted analytically to the HF-MM difference to determine the magnitude of V_1 , V_2 and V_3 .

To permit a detailed sampling of conformational space at reasonable computational cost, geometries were first optimised semi-empirically (MNDO/d) in all cases, followed by a single point calculation at the HF level (HF/STO-3G*). Calculation of relative ground state and transition state energies of some of the simpler compounds by DFT (B3LYP) using a higher precision basis set (6-311G**) gave virtually identical values (see ESI†). As MNDO/d is not parameterised for selenium compounds (in HYPERCHEM), the selenium parameters were obtained by scaling the equivalent sulfur values according to the difference in atomic radius between sulfur and selenium.

A list of all parameters which have been modified or added to the MM+ force field in HYPERCHEM¹⁸ are given in the ESI.†

Triaryl (2-RC₆H₄)₃PX derivatives

Members of the 2-MeC₆H₄ and 2-CF₃C₆H₄ triaryl series **1a–e** and **2a,b** have previously been characterised both in the solid state and in solution (throughout, **a** denotes phosphine, **b**, **c** and **d** denote phosphine oxide, sulfide and selenide respectively and **e** denotes the Cr(CO)₅ complex).^{19,20} (2-EtC₆H₄)₃P **3a** and (2-ⁱPrC₆H₄)₃P **4a** were prepared by reaction of PCl₃ with 2-EtC₆H₄Li and 2-ⁱPrC₆H₄MgBr respectively. Only a single 2-^tBuC₆H₄ substituent could be introduced through the reaction of (2-MeC₆H₄)₂PCl with 2-^tBuC₆H₄MgI to give (2-MeC₆H₄)₂(2-^tBuC₆H₄)P **5a**. The diaryl derivatives (2-MeC₆H₄)₂MeP **6a** and (2-MeC₆H₄)₂^tBuP **7a** were prepared by reaction of (2-MeC₆H₄)₂PCl with MeLi and ^tBuPCl₂ with 2-MeC₆H₄Li respectively. Oxide, sulfide, selenide

and Cr(CO)₅ derivatives were prepared by established methods (see Experimental section).

The structure and stereodynamics of tris(*o*-alkyl)phosphines and their derivatives

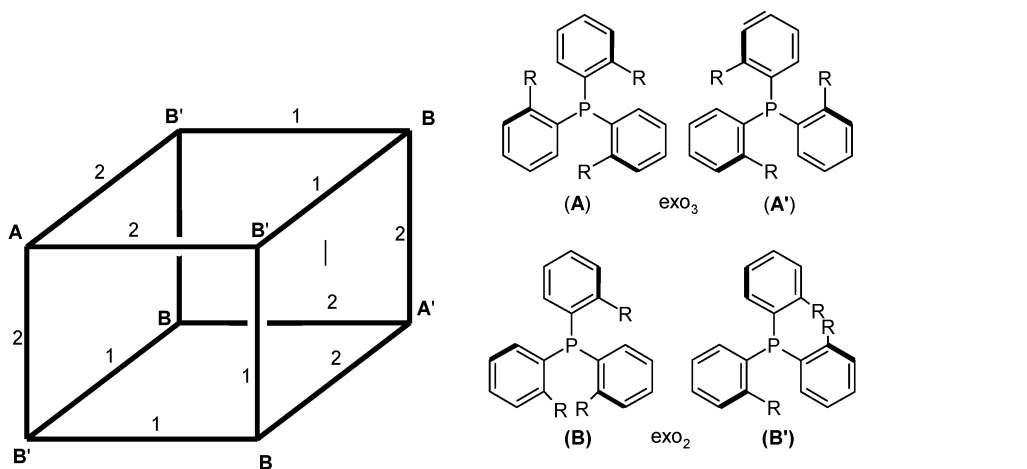
Triarylphosphines often adopt a chiral, helical conformation. Differing ring substituents may introduce central chirality at the phosphorus atom, and molecules may also differ in the arrangement of ring substituents with respect to a reference plane defined by the three *ipso* carbon atoms.

Correlated phosphorus-ring rotation has previously been observed for the 2-Me and 2-CF₃ derivatives^{19,20} and is a general feature of molecular propellers of the types Ar₃Z and Ar₃ZX.^{21a,b} Crystal structures of (2-MeC₆H₄)₃PX compounds²² show either an *exo*₃ or an *exo*₂ conformation of the aryl rings (see Scheme 1 for conformer nomenclature). On the assumption that only these two conformers are populated, P–C rotational isomerism for an Ar₃PX compound *via* 1-, 2- and 3-ring flip mechanisms may be represented as in Scheme 1. The 1-, 2- and 3-ring flip intermediates of idealised structures **I** to **V** are required for conformer interconversion along edges and diagonals. Four conformers [**A**,**B**] and their helical enantiomeric equivalents [**A'**, **B'**] are possible.

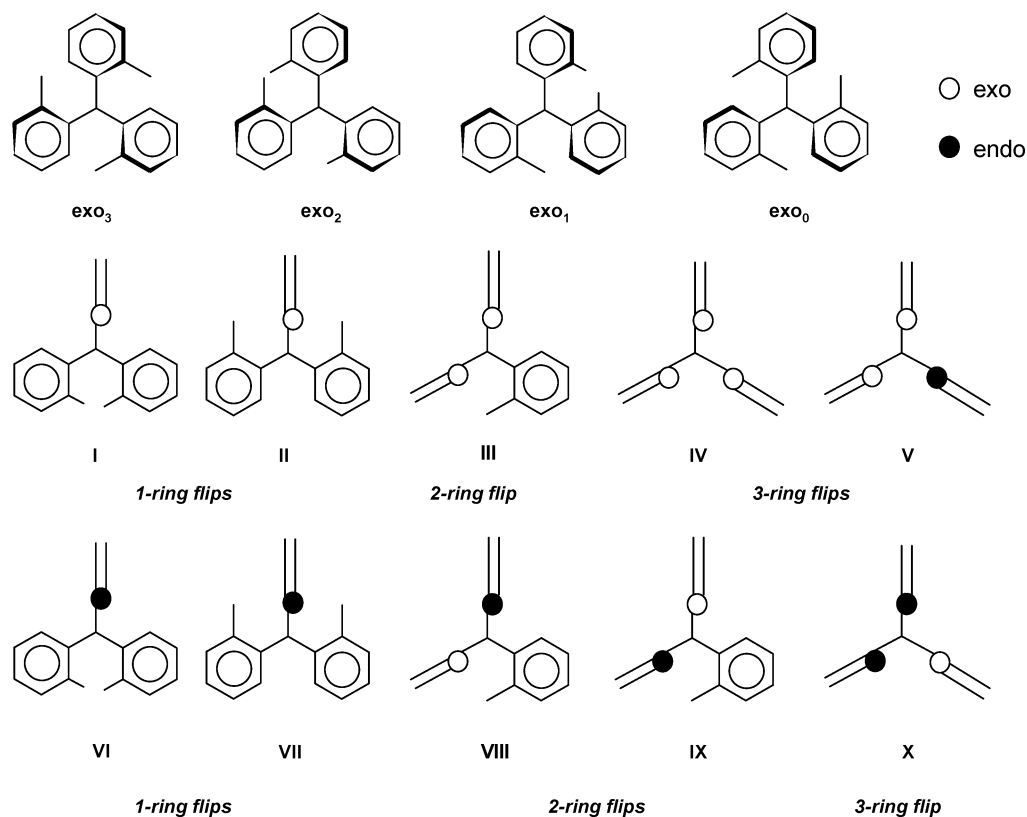
Using the adapted force field, a complete MM analysis for (2-MeC₆H₄)₃PO **1b** was performed using a systematic driver calculation to fully explore conformational space with respect to the three ring torsions. The methyl substituents adjust easily to differing ring conformations, and were not analysed as an additional variable. The resulting conformational energy surface is thus four-dimensional, combining three ring torsions with the calculated steric energy. The minimum energy in each data series may be identified, thus permitting correlation with the corresponding angle values to generate a map of energy minima suitable for the identification of conformers and lowest energy interconversion pathways. Fig. 1 displays two contour maps correlating two of these torsional angles with energy in the most important regions of the energy surface.

These maps show energy minima for the *exo*₃, *exo*₂ and *exo*₁ conformers. The map identifies the transition state **III** to lie along the lowest energy path of *exo*₂/*exo*₃ exchange, a process which is accompanied by ring exchange and a reversal of helicity. The transition state **IV** lies along the path which represents helix inversion in the *exo*₃ isomer. Both 1-ring flip pathways which invert helicity and exchange rings in the *exo*₂ conformer may be identified, with that occurring *via* transition state **II** representing the lower energy alternative. However, a sequence of 2- and 3-ring flips appears to be the most likely process for *exo*₂ helix inversion on this conformational energy surface. The *exo*₁ conformer may also be identified as a local energy minimum, whereas the *exo*₀ conformer is higher in energy and obscured by part of the *exo*₁ surface. The geometries of calculated transition states are close to those of the idealised structures.

As the detailed analysis of **1b** accurately reproduced the ground state solid state structure and the conformer distribution and P–C rotational barriers in solution, a less intensive computational approach was adopted for other derivatives in which ground state conformations were explored by 1000 iteration conformational



Numbers on vertex edges indicate the ring flip mechanism interconverting the vertex structures. Diagonally opposite vertices are connected by a 3-ring flip



Scheme 1 Ring flip mechanism for triarylphosphine.

searches and ring flip barriers were calculated using the geometries of the idealised transition states (shown in Scheme 1).

The crystal structures of **1a**, **2a**^{13,14} and **3a** to **5a** (Fig. 2) also show *exo*₃ conformations of the aryl rings. In **5a**, the 2-^tBuC₆H₄

ring is much closer to collinearity with the P-lone pair axis, whilst the remaining 2-MeC₆H₄ rings are flattened to some degree to compensate. As with **1a** and **2a**, ³¹P NMR spectra of **3a** to **5a** are temperature invariant down to 163 K, indicating an exclusive

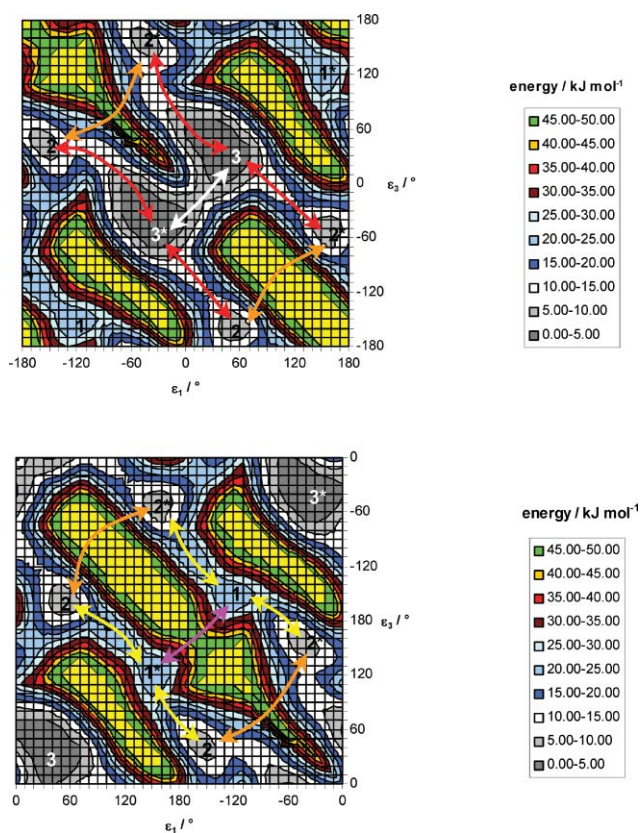


Fig. 1 3-Dimensional energy graphs for **1b**.

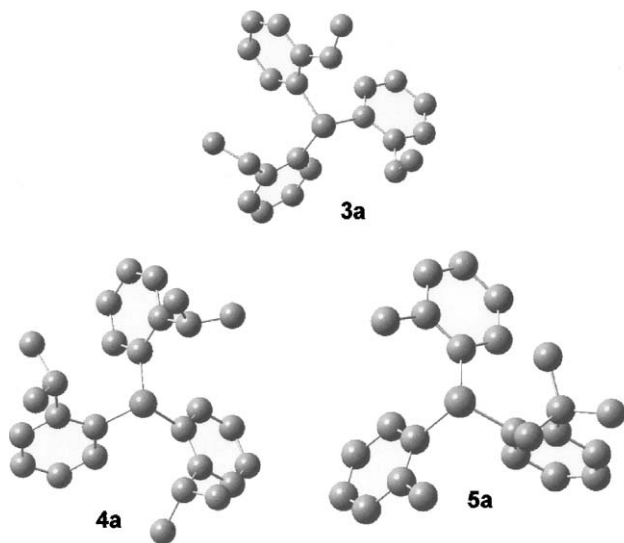


Fig. 2 Solid state structures of **3a**, **4a** and **5a** (hydrogens omitted).

population of the exo_3 conformer.[§] The higher energy process which results in helix inversion is NMR silent for **1a** and **2a**, but may be observed and the barrier quantified through line shape analysis in the variable temperature behaviour of the ^1H CH_2CH_3 resonances of **3a**, the CHMe_2 resonances of **4a** and the $o\text{-Me}$

[§] The characteristic^{11a} high field resonance of H_6 (6.7–6.8 ppm) is consistent only with exo_3 .

resonances of **5a**; these become diastereoisotopic in the presence of helix inversion which is slow on the NMR timescale.

Except for **5b** and **1e**, experimental barriers and conformer populations for the exo_2/exo_3 exchange process for the oxides, sulfides and selenides may be obtained from the variable temperature ^{31}P NMR spectra which show two resonances at low temperature assignable to the exo_3 and exo_2 conformers.[¶] Barriers for helix inversion may be obtained from line shape analyses of the higher temperature ^1H spectra where possible. The ^{31}P spectra of **5b** and **1e** are temperature invariant, implying a single conformer in solution. The crystal structure of **5b** (Fig. 3) shows that this may be described as exo_3 , albeit highly distorted in terms of the ring torsion angles, whereas that of **1e** (Fig. 3) is clearly exo_2 .

Agreement between calculated and observed P-ring torsional angles in the solid state is excellent (Table 1). Given the substantial variation of conformational equilibrium constant with temperature for many of the compounds, and given the usual difficulties of comparing calculated relative stabilities in the gas phase at zero Kelvin with solution values at non-zero temperatures, the agreement between calculated and experimental thermodynamic parameters is good (Table 1). The standard deviation of the relative percent difference between calculated and experimental rotational barriers for the eleven barriers shown in Table 1 ($\pm 10\%$) is the same as the approximate precision of the measurement of the enthalpy of activation from the NMR spectra.

The exo_3 conformation becomes increasingly less favourable relative to exo_2 as the size of the phosphorus substituent X is increased; exo_2 is calculated to be the most stable conformer for $\text{X} = \text{Se}$, $\text{Cr}(\text{CO})_5$, though at no stage do exo_1 or exo_0 become the global minimum. The idealised 2-ring flip transition state **III** represents the lowest energy exchange process for exo_2/exo_3 exchange. This transition state, and that for 3-ring flip helix inversion in the exo_3 conformer (**IV**), have two or three rings respectively which are exo and perpendicular to the reference plane; the energies of these transition states increase as the size of the X substituent increases. In contrast, the energies of the 1-ring flip transition states, which contain only a single perpendicular exo ring, are calculated to remain constant or decrease slightly from the oxide to the selenide. For **1e**, there is also good agreement regarding the orientation of the phosphine relative to the $\text{Cr}(\text{CO})_4$ plane (Fig. 2), and the calculated magnitude of the Cr–P rotational barrier (26 kJ mol^{-1}) is close to that observed experimentally from line broadening of the CO resonance ($\leq 32 \text{ kJ mol}^{-1}$). The lowest energy process for ring exchange for **1e** is calculated to be a sequential series of 1-ring flips which exchanges rings in the exo_2 conformer without conformer interconversion.

Ring-substituent rotational profiles may also be investigated by MM calculation (Table 2). For example, the energy profile for ring- ^1Bu rotation in the exo_3 isomer of **5b** shows a 3-fold symmetry with three equivalent global minima in which the P=O bond bisects the angle between two methyl groups. This is observed in the solid state structures of **5a,b** (Fig. 2, 3). Probably as a result of steric destabilisation of the ground state, the predicted rotational barriers for **5a** and **5b** are surprisingly low (9 and 14 kJ mol^{-1}), and

[¶] The major conformer may be assigned on the basis of the multiplicity of the resonance for the major conformer observed in the ^1H or ^{19}F subspectrum for the $o\text{-Me}$ or $o\text{-CF}_3$ substituent (one for exo_3 , three for exo_2).

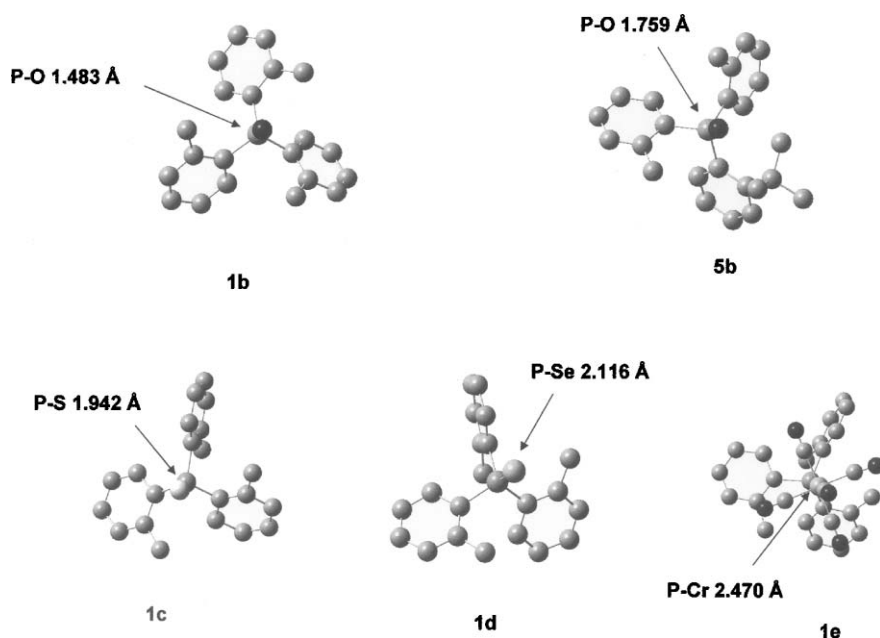


Fig. 3 Solid state structures of **1b**–**e** and **5b** (hydrogens omitted).

in agreement, no broadening of the ^1Bu resonance is observed in the ^1H NMR of either **5a, b** down to 163 K. As predicted, the solid state structures of the ethyl and isopropyl compounds **3a** and **4a** place the methyl substituents pointing away from the P-lone pair axis.

The structure and stereodynamics of alkyldiarylphosphines and their derivatives

Conformational isomerism in ring substituted alkyldiarylphosphines Ar_2PR and their derivatives may be analysed in the same topological manner (Scheme 2). Thus, where $\text{Ar} = 2\text{-MeC}_6\text{H}_4$ **6a**–**e**, the four possible conformers exo_2 , $exo_{1a,b}$ and exo_0 (and their corresponding enantiomers of opposite helicity) may be identified. For alkyldiaryl derivatives, systematic variation of the two ring torsion angles permits generation of a three-dimensional energy surface, thus facilitating a direct analysis of conformational preferences and interconversion mechanisms. This is fortunate, since for these sterically more flexible compounds, calculations of rotational barriers using idealised transition states do not accurately reproduce experimental data. Ground state conformational preferences were explored in detail by 1000 iteration conformational searches, allowing free adjustment of the Me or ^1Bu group. For the P–Me series **6a**–**e**, agreement between predicted and observed solid state structures for **6b, c, e** is also good (Table 3, Fig. 4). Three-dimensional plots are shown in Fig. 5 and 6 for the phosphines and for their $\text{Cr}(\text{CO})_5$ complexes, whilst key calculated structural, kinetic and thermodynamic data are summarized in Table 3.

Though the lowest energy structure for **6b** is calculated to be exo_2 , the compound crystallises as the exo_1 conformer. The calculated energy difference, however, is sufficiently small to be due to crystal packing forces. For **6e**, agreement between the predicted and observed orientation of the ligand relative to the $\text{Cr}(\text{CO})_4$

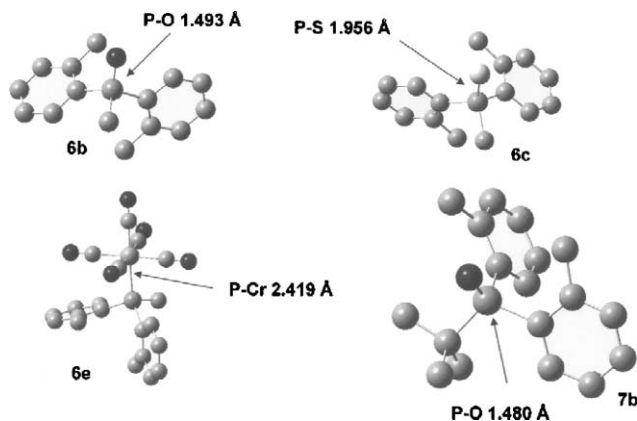


Fig. 4 Solid state structures of **6b, c, e** and **7b**.

plane is also excellent. Only the $\text{Cr}(\text{CO})_5$ derivative **6e** exhibits low temperature limiting ^1H NMR spectra. This may be taken as indicating restricted ring exchange *via* slowing of P–C rotation in exclusively the exo_{1a} isomer, since ^{31}P spectra are independent of temperature over the same range. The calculated barrier for direct helix exchange in the exo_{1a} isomer is much higher than that observed experimentally, and a more likely scenario involves interconversion of exo_{1a} with exo_2 accompanied by helix inversion in the exo_2 conformer.

For the more sterically demanding ^1Bu series **7a**–**e**, low temperature limiting spectra can be obtained for all but the phosphine itself **7a**. For **7b**–**e**, ^{31}P spectra are resolved into two resonances assignable to exo_2 and exo_{1a} with the relative amount of exo_2 decreasing across the series. This is in agreement with the calculation of relative stability for both the ^1Bu and Me series. As intuitively expected on steric grounds, the exo_2 isomer is stabilised

Table 1 Comparison of calculated and experimental structural, thermodynamic and kinetic data for triarylphosphines and their derivatives

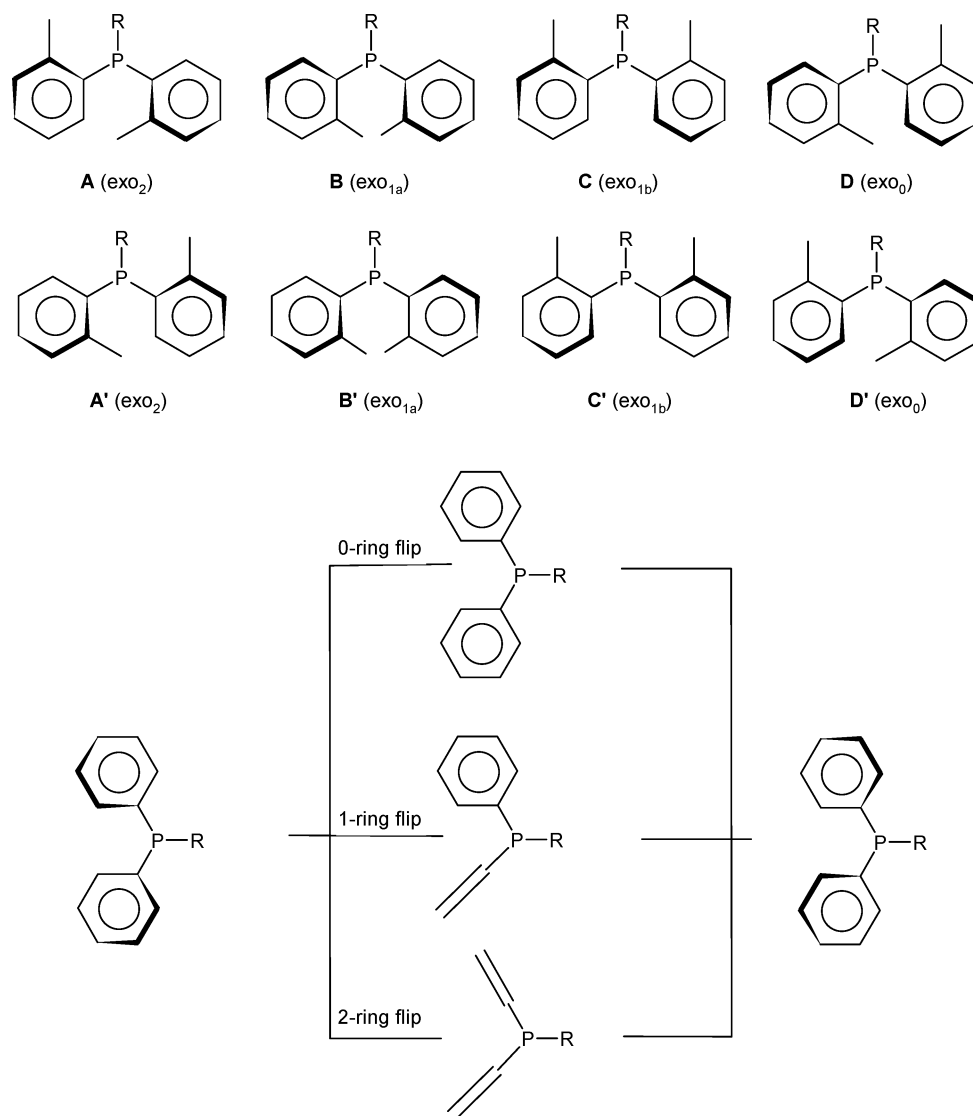
	a	b	c	d	e
1					
\sum^a	39 ± 3 (43 ± 3)	40 ± 3 (46 ± 4)	−161, 51, 56 (−163, 57, 57)	−164, 54, 56 (−168, 60, 54)	−180, 73, 56 (−179, 70, 60)
exo_3^b	0 (<i>exo_3</i> only)	0 (0)	0 (4.3, 173 K)	0.2 (4.6, 163 K)	25.1
exo_2	9.0	6.4 (2.4, 163 K)	1.0 (0)	0 (0)	0 (<i>exo_2</i> only)
exo_1	24.6	19.8	8.9	7.0	0.8
exo_0	42.3	33.5	19.1	17.5	12.1
1-ring _a (I)	122.1	128.4	106.4	103.1	104.1
1-ring _b (II)	51.3	53.6	44.6	41.9	44.3 (39)
2-ring (I)	11.7	19.1 (30)	33.7 (38)	38.7 (40)	90.8
3-ring _a (III)	29.6	38.7	82.7	98.4	220.0
3-ring _b (IV)	74.3	80.0	112.5	123.1	201.7
2					
\sum^a	39 ± 1 (35 ± 2)	37 ± 1 (42 ± 7)			
exo_3^b	0 (<i>exo_3</i> only)	0 (0)			
exo_2	9.0	6.4 (4.0, 163 K)			
exo_1	24.6	19.8			
exo_0	42.3	33.5			
1-ring _a (II)	122.1	128.4			
1-ring _b (III)	51.3	53.6			
2-ring (I)	11.7	19.1 (34)			
3-ring _a (IV)	29.6	38.7			
3-ring _b (V)	74.3	80.0			
3					
\sum^a	39 ± 0 (41 ± 6)	45, 41, 36			
exo_3^b	0 (<i>exo_3</i> only)	0 (1.4, 173 K)			
exo_2	11.0	4.8 (0)			
exo_1	29.6	23.5			
exo_0	57.2	40.6			
1-ring _a (II)	133.7	151.3			
1-ring _b (III)	70.1	69.8			
2-ring (I)	19.0	27.2 (33/36)			
3-ring _a (IV)	33.9 (46)	49.0			
3-ring _b (V)	81.2	90.1			
4					
\sum^a	38 ± 16 (43 ± 3, 40 ± 9) ^c	47 ± 2	−173, 58, 59	−174, 59, 60	
exo_3^b	0 (<i>exo_3</i> only)	0 (3.7, 173 K)			
exo_2	7.2	2.1 (0)	0 (<i>exo_2</i> only)	4.1	
exo_1	29.5	25.0	16.1	26.0	
exo_0	51.0	37.1	37.1	26.0	
1-ring _a (II)	143.7	194.8	194.8	134.7	
1-ring _b (III)	58.8	61.1	58.1 (55)	57.9 (50)	
2-ring (I)	15.8	32.3 (39)	57.9 (50)	133.3	
3-ring _a (IV)	34.1 (47)	65.4 (53)	103.8	155.7	
3-ring _b (V)	84.2	103.8			
5					
\sum^a	23, 47, 47 (38, 35, 48)	38, 35, 48 (39, 39, 54)			
exo_3	0 (<i>exo_3</i> only)	0 (<i>exo_3</i> only)			
exo_{2a}	14.2	10.5			
exo_{2b}	16.3	9.5			
exo_{2c}	48.9	33.6			
exo_{1a}	29.5	24.4			
exo_{1b}	57.1	42.3			
exo_{1c}	69.6	52.7			
exo_0	97.4	70.5			
1-ring _a	157.2	157.1			
1-ring _{a'}	121.4	129.6			
1-ring _b	98.4	89.1			
1-ring _{b'}	63.1	65.8			
2-ring _a	39.6	38.2			
2-ring _b	21.6	29.7			
2-ring _c	21.1	30.9			
3-ring _a	47.8 (54)	57.4 (73)			
3-ring _b	142.5	146.8			
3-ring _{b'}	86.9	94.6			

^a P-ring torsional angles (°); observed solid state values are in parentheses. ^b Relative energies (kJ mol^{−1}); experimental values from variable temperature NMR are given in parentheses. ^c Two molecules in unit cell.

Table 2 Calculated and observed structural and kinetic data for ring-substituent orientation

	av. $ \tau_{\text{subst}} ^a / ^\circ$				Barrier to substituent rotation/kJ mol ⁻¹			
	<i>exo</i> ₃	<i>exo</i> _{2a}	<i>exo</i> _{2b}	<i>exo</i> _{2c} ^b	<i>exo</i> ₃	<i>exo</i> _{2a}	<i>exo</i> _{2b}	<i>exo</i> _{2c} ^b
3a ^c	84 (<i>121</i>)		<i>exo</i> ₂ : 100		23		<i>exo</i> : 26, ^d <i>endo</i> : 56	
3b ^c	97		<i>exo</i> ₂ : 103		32		<i>exo</i> : 34, ^d <i>endo</i> : 56	
4a ^c	8 (<i>5, 4</i>) ^e		<i>exo</i> ₂ : 12		32		<i>exo</i> : 40, ^d <i>endo</i> : 67	
4b ^c	10		<i>exo</i> ₂ : 10		43		<i>exo</i> : 47, ^d <i>endo</i> : 66	
4c ^c	9		8		54		<i>exo</i> : 56, ^d <i>endo</i> : 68	
5a	179 (<i>177</i>)	179	176	164	9	9	7	24
5b	166 (<i>168</i>)	166	163	164	14	14	9	24

^a Ring-substituent torsional angles. Observed solid state values are given in parentheses. ^b Substituent *endo*. ^c *exo*₂ conformations indistinguishable. ^d Lower barrier. ^e Two molecules in unit cell.

**Scheme 2** Ring flip mechanism for alkyldiarylphosphine.

relative to *exo*_{1a} more in the ¹Bu series than in the methyl series. Thus, whereas **6b** has an *exo*_{1a} solid state structure, that of **7b** is *exo*₂ (Fig. 4).

All the calculated barriers for P-CH₃ rotation in the lowest energy conformers of **6a–d** lie below the limit of NMR measurement, and no decoalescence of the ¹H P-Me resonance is observed.

In contrast, barriers for P-¹Bu rotation in **7b–d** are substantially higher, and calculated barriers are in good agreement with those measured by variable temperature NMR. The crystal structure of the oxide **7b** (Fig. 4) confirms the predicted lowest energy conformation of the ¹Bu substituent in which the P=O bond bisects a pair of methyl groups.

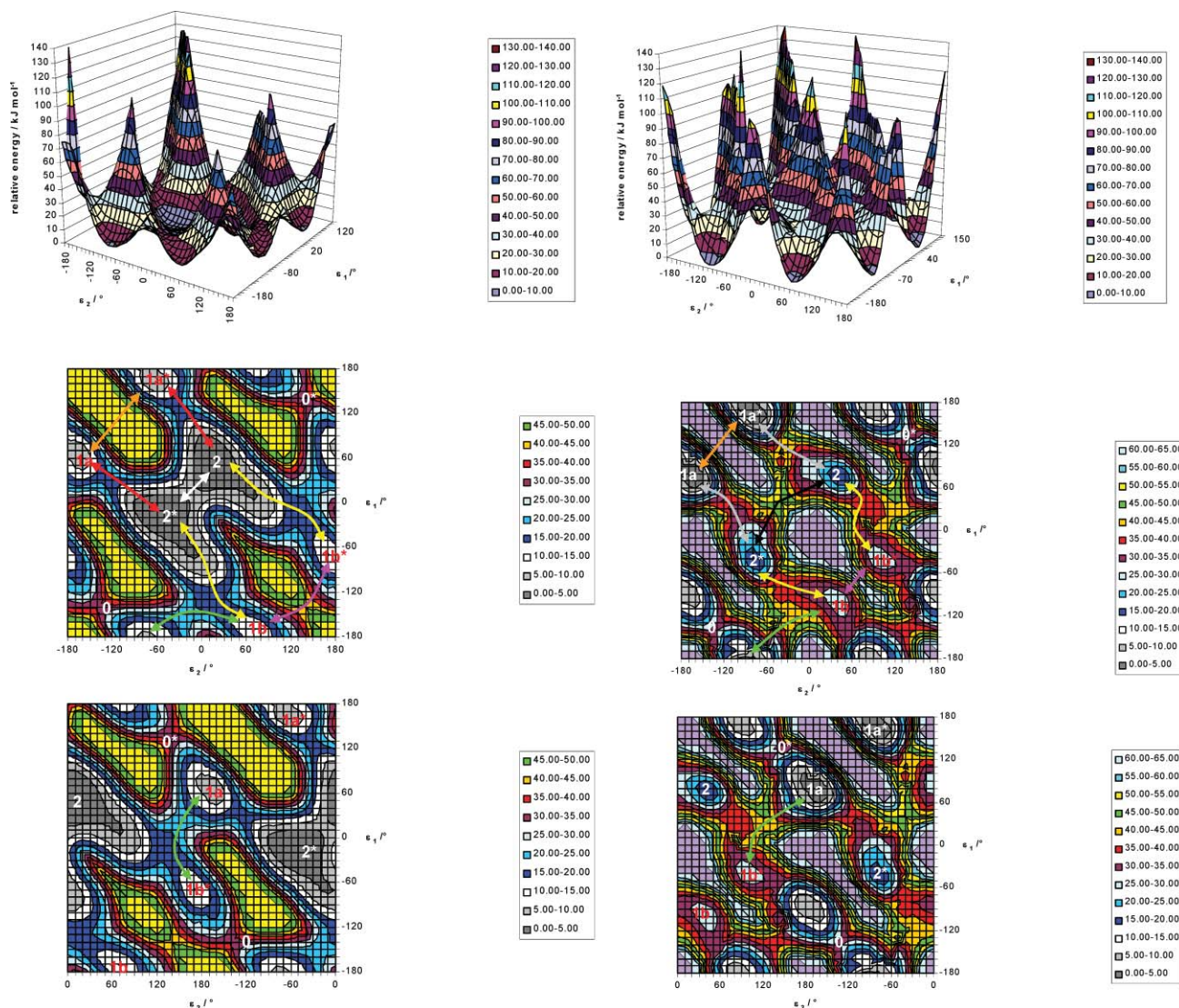


Fig. 5 3-Dimensional energy graphs for **6a** (left), **e** (right).

Conclusions

A force field has been developed which can accurately reproduce relative conformer stabilities and rotational barriers for triaryl- and diarylalkyl phosphines and their chalcogenide and $\text{Cr}(\text{CO})_5$ derivatives. Further work is in progress on the application of this force field to the modelling of bidentate phosphines and their chalcogenide and $\text{Cr}(\text{CO})_4$ complexes.

Experimental

Reactions involving lithium and magnesium reagents were conducted under argon. Except for the preparation of phosphine oxides, reactions were conducted under dinitrogen. NMR spectra were recorded using a Bruker DPX300 spectrometer (^1H , 300 MHz; ^{13}C , 75 MHz; ^{31}P , 121 MHz). Full NMR data for all compounds are provided in the ESI.†

Temperatures were measured using the in-built copper–constantan thermocouple which had previously been calibrated with a platinum resistance thermometer. Line shape analyses of

NMR spectra were performed by computer simulation. For the case of two exchanging nuclei, an in-house program based on the equation of Sutherland²³ was used. For greater numbers of nuclei, a program written by R. E. D. McClung (University of Alberta, Canada) was adapted for use. Full data obtained from the line shape analyses can be found in the ESI.†

Syntheses

1. Synthesis of $2\text{-}^i\text{PrC}_6\text{H}_4\text{Br}$. Aqueous HBr (65 ml, 48%) was added rapidly to a mechanically stirred refluxing solution of $2\text{-}^i\text{PrC}_6\text{H}_4\text{NH}_2$ (17.2 g, 128 mmol) in water (160 ml). After refluxing for 30 minutes, the solution was cooled to 0 °C and a solution of NaNO_2 (8.8 g, 127 mmol) in water (45 ml) was added, maintaining the temperature between 0 and 5 °C. The cold solution of the diazonium salt was added rapidly to a stirred solution of CuBr (21.0 g, 147 mmol), aqueous HBr (43 ml, 48%) and water (120 ml). After stirring at room temperature for 20 minutes, the mixture was heated on a steam bath for 1 hour and then steam distilled. The distillate was extracted with diethyl ether (300 ml), washed with

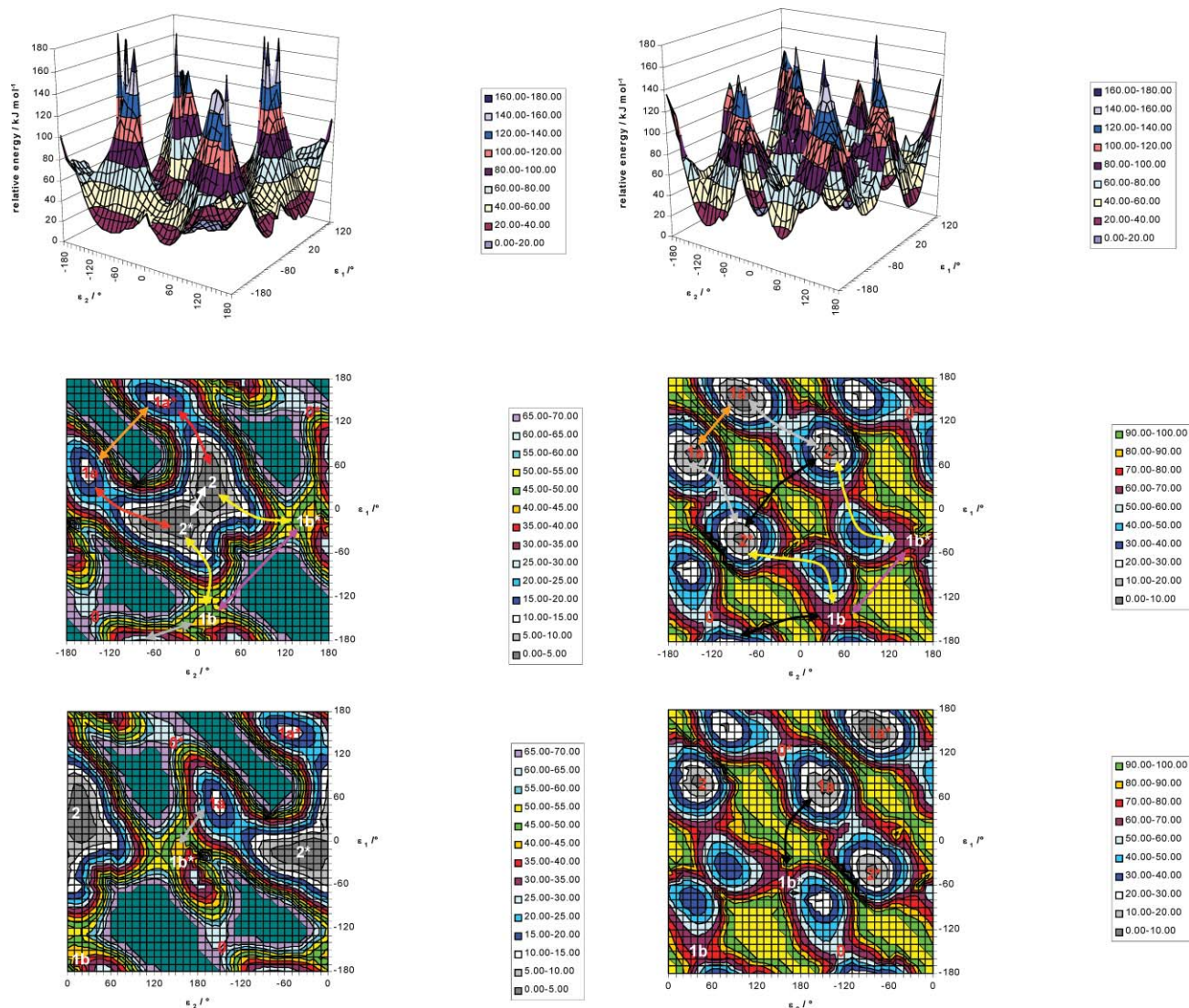


Fig. 6 3-Dimensional energy graphs for **7a** (left), **e** (right).

water and dried over MgSO_4 . After removal of solvent, the residue was purified by column chromatography [silica, petroleum ether (bp 40–60 °C)] to give the product (15.3 g, 60%) as a colourless liquid from the fastest moving fraction.

2. Synthesis of $2\text{-}^i\text{BuC}_6\text{H}_4\text{I}^{25}$. $2\text{-}^i\text{BuC}_6\text{H}_4\text{NH}_2$ (22 g, 147 mmol) was added to 3.4 M H_2SO_4 (20 ml) and cooled to -10 °C. A saturated aqueous solution of NaNO_2 (10.5 g, 152 mmol) was added with vigorous stirring over 5 minutes to give a light brown slurry. After stirring for a further hour at -10 to 0 °C, the slurry of the diazonium salt was added rapidly to a concentrated ice-cold solution of KI (75 g, 0.45 mol). After stirring at 0 °C for 2 hours, the suspension was extracted with diethyl ether (150 ml). After removal of solvent, purification by column chromatography [silica, petroleum ether (bp 40–60 °C)] gave the product (22.8 g, 60%) as a colourless liquid from the fastest moving fraction.

3. Synthesis of $(2\text{-EtC}_6\text{H}_4)_3\text{P}$ (3a**).** $2\text{-EtC}_6\text{H}_4\text{Li}$ was prepared by addition of $^n\text{BuLi}$ (16.9 ml of 1.6 M solution in hexane,

27.0 mmol) to a solution of $2\text{-EtC}_6\text{H}_4\text{Br}$ (5.0 g, 27.0 mmol) in dry diethyl ether (30 ml) at -5 °C. After stirring for 1 hour, PCl_3 (1.13 g, 8.19 mmol) in diethyl ether (15 ml) was added dropwise at 0 °C over 15 minutes. The solution was warmed to room temperature and stirred for a further hour. After filtration and removal of solvent, the residue was purified by column chromatography [silica, petroleum ether (bp 60–80 °C)] and recrystallised from petroleum ether (bp 60–80 °C) to give **3a** as white crystals (1.7 g, 57%); mp $98\text{--}99$ °C (Found: C, 83.2; H, 7.79%. $\text{C}_{24}\text{H}_{27}\text{P}$ requires C, 83.2; H, 7.80%).

4. Synthesis of $(2\text{-}^i\text{PrC}_6\text{H}_4)_3\text{P}$ (4a**).** A solution of $2\text{-}^i\text{PrC}_6\text{H}_4\text{MgBr}$ was prepared by addition of $2\text{-}^i\text{PrC}_6\text{H}_4\text{Br}$ (5.0 g, 22.2 mmol) to magnesium turnings (0.54 g, 22.3 mmol) in tetrahydrofuran (10 ml) using 1,2-dibromoethane as initiator. The rate of reaction was controlled by the addition of a further 40 ml of tetrahydrofuran. After refluxing for 2 hours and cooling to 0 °C, PCl_3 (0.78 g, 5.69 mmol) in tetrahydrofuran (10 ml) was added dropwise. After stirring at room temperature for 2 hours, the solution was heated to 50 °C for a further 2 hours. After

Table 3 Calculated and experimental structural, thermodynamic and kinetic data for diarylalkylphosphines and their derivatives

	a	b	c	d	e
6					
\sum^a	60, 13	62, -162 (54 , -174)	67, -163 (66 , -174)	70, -164	81, -163 (81 , -152)
exo_2^b	0	exo_{1a} 0	exo_{1a} 1.4	exo_{1a} 2.9	exo_{1a} 15.6
exo_{1a}	6.5	4.8	0	0	0 (<i>exo_{1a}</i> only)
exo_{1b}	33.9	8.7	4.2	4.6	26.1
exo_0	33.9	30.5	22.3	21.1	12.8
exo_2 (helix inversion)	5.8	6.5	16.9	16.2	49.7 (47)
exo_{1a} (helix inversion)	129.3	133.0	99.7	99.1	125.8
exo_{1b} (helix inversion)	44.3	43.1	36.9	35.2	66.7
exo_2/exo_{1a}	18.1	15.8	12.0	12.3	37.7
exo_2/exo_{1b}	18.4	18.9	18.0	18.7	35.6
exo_{1a}/exo_{1b}	20.4	21.9	22.6	22.3	41.8
CH ₃ rotational barrier	11.3	14.9 (exo_2), 11.7 (exo_{1a})	13.0	12.9	9.7
7					
\sum^a	22, 15	35, 16 (51 , 18)	75, 22	77, 23	81, -159
exo_2^b	0	exo_2 0 (0)	exo_2 0 (2.9 , 173 K)	exo_2 0 (4.3 , 203 K)	exo_{1a} 7.2 (3.0 , 313 K)
exo_{1a}	13.0	8.7 (2.6 , 173 K)	3.2 (0)	2.2 (0)	0 (0)
exo_{1b}	41.6	40.2	45.8	46.4	68.9
exo_0	60.4	56.2	54.1	53.5	56.6
exo_2 (helix inversion)	5.3	10.9	26.5 (55)	36.0 (64)	105.0
exo_{1a} (helix inversion)	131.9	134.0	97.6	95.8	111.1
exo_{1b} (helix inversion)	132.4	212.2	97.5	91.9	188.4
exo_2/exo_{1a}	20.6	18.1 (33)	19.8 (41)	21.7 (42)	54.0 (68)
^t Bu rotational barrier	13.3	21.2 (36)	46.3 (42)	46.9 (42)	29.8 (35 , exo_{1a} : 38 , exo_2)

^a P-ring torsional angle (°); observed solid state values are in parentheses. ^b Relative energies (kJ mol⁻¹); experimental values measured by variable temperature NMR are in parentheses.

cooling, water (2 ml) was added carefully. Removal of solvent and recrystallisation from ethanol gave **4a** as white crystals (1.3 g, 59%); mp 108–110 °C (Found: C, 83.5; H, 8.50%. C₂₇H₃₃P requires C, 83.5; H, 8.57%).

5. Synthesis of (2-MeC₆H₄)₂(2-^tBuC₆H₄)P (5a**).** 2-^tBuC₆H₄I (2.26 g, 8.67 mmol) in tetrahydrofuran (40 ml) was added to magnesium turnings (0.22 g, 9.0 mmol). After stirring at reflux for 7 hours, only a small amount of magnesium remained unreacted. After cooling to 0 °C, (2-MeC₆H₄)₂PCl (2.10 g, 8.67 mmol) in tetrahydrofuran (30 ml) was added slowly over 30 minutes. The reaction was stirred overnight at room temperature and water (1 ml) was added carefully. After removal of solvent, the residue was purified by column chromatography [silica, 9 : 1 petroleum ether (bp 40–60 °C)–dichloromethane] followed by recrystallisation from petroleum ether (bp 60–80 °C) to give **5a** as white crystals (0.56 g, 17%); mp 150–153 °C (Found: C, 83.3; H, 7.87%. C₂₄H₂₇P requires C, 83.2; H, 7.80%).

6. Synthesis of (2-MeC₆H₄)₂MeP (6a**).** MeLi (26.5 ml of a 1.4 M solution in hexane, 37.1 mmol) was added to a stirred solution of (2-MeC₆H₄)₂PCl (9.12 g, 36.7 mmol) in diethyl ether (50 ml) at -40 °C. After stirring for 1 hour, the solution was warmed to room temperature and stirred overnight. After addition of saturated NH₄Cl solution (5 ml), the product was extracted with diethyl ether (60 ml). After removal of solvent, the crude product was purified by vacuum distillation (100 °C, 0.01 mmHg) to give **6a** as a white solid (3.9 g, 85%); mp 53–55 °C (Found: C, 79.3; H, 7.38%. C₁₅H₁₇P requires C, 79.0; H, 7.52%).

7. Synthesis of (2-MeC₆H₄)₂^tBuP (7a**).** ⁿBuLi (59.9 ml of a 2.5 M solution in hexane, 150 mmol) was added dropwise to a

stirred solution of 2-MeC₆H₄Br at -50 °C. After warming to room temperature, the solution was stirred for a further 3 hours. After cooling to -10 °C, ^tBuPCl₂ (7.0 g, 44 mmol) in diethyl ether (50 ml) was added over 30 minutes. The solution was stirred overnight and finally refluxed for 30 minutes. After addition of water (2 ml) and removal of solvent, the residue was purified by column chromatography [silica, petroleum ether (bp 40–60 °C)] and recrystallised from methanol to give **7a** as white crystals (9.8 g, 83%); mp 86–88 °C (Found: C, 79.8; H, 8.87%. C₁₈H₂₃P requires C, 80.0; H, 8.59%).

8. Synthesis of (2-MeC₆H₄)₂MePO (6b**).** A solution of *m*-chloroperbenzoic acid (0.3 g, 1.97 mmol) in toluene (15 ml) was added dropwise to a stirred solution of (2-MeC₆H₄)₂MeP (0.3 g, 1.3 mmol) in toluene (10 ml). After stirring for 12 hours, the solution was washed with 10% Na₂CO₃ solution (30 ml). After drying with MgSO₄ and removal of solvent, the residue was recrystallised from petroleum ether (bp 60–80 °C) to give **6b** as a white solid (0.3 g, 97%). Other phosphine oxides were prepared in a similar manner.

(2-MeC₆H₄)₂MePO. Mp 126–127 °C (Found: C, 73.8; H, 7.20%. C₁₅H₁₇OP requires C, 73.9; H, 7.02%).

(2-MeC₆H₄)₂^tBuPO. Mp 134–136 °C (Found: C, 75.7; H, 8.27%. C₁₈H₂₃OP requires C, 75.5; H, 8.11%).

(2-EtC₆H₄)₃PO. Mp 164–166 °C (Found: C, 79.1; H, 7.43%. C₂₄H₂₇OP requires C, 79.6; H, 7.46%).

(2-ⁱPrC₆H₄)₃PO. Mp 198–202 °C (Found: C, 80.4; H, 8.79%. C₂₇H₃₃OP requires C, 80.3; H, 8.24%).

(2-MeC₆H₄)₂(2-^tBuC₆H₄)PO. Mp 186–188 °C (Found: C, 79.8; H, 7.62%. C₂₄H₂₇OP requires C, 79.6; H, 7.46%).

9. Synthesis of (2-MeC₆H₄)₂MePS (6c). Sulfur (0.1 g, 3.2 mmol) and (2-MeC₆H₄)₂MeP (0.3 g, 1.3 mmol) were refluxed in CS₂ (15 ml) for 4 hours. Removal of solvent, followed by purification by preparative tlc (silica, CH₂Cl₂) and recrystallisation from ethanol gave **6c** as white crystals (0.2 g, 44%). Other phosphine sulfides were prepared in a similar manner.

(2-MeC₆H₄)₂MePS. Mp 146–148 °C (Found: C, 69.4; H, 7.01%. C₁₅H₁₇PS requires C, 69.2; H, 6.54%).

(2-MeC₆H₄)₂^tBuPS. Mp 137–138 °C (Found: C, 71.4; H, 7.79%. C₁₈H₂₃PS requires C, 71.5; H, 7.68%).

(2-ⁱPrC₆H₄)₃PS. Mp 120–122 °C (Found: C, 77.5; H, 7.99%. C₂₇H₃₃PS requires C, 77.2; H, 7.92%).

10. Synthesis of (2-MeC₆H₄)₂MePSe (6d). A solution of (2-MeC₆H₄)₂MeP (0.5 g, 2.19 mmol) in CHCl₃ (10 ml) was refluxed overnight with selenium powder (0.5 g, 6.64 mmol). The suspension was filtered through Celite and the solvent removed. Recrystallisation from ethanol gave white crystals of **6d** (0.5 g, 74%). Other phosphine selenides were prepared in a similar manner.

(2-MeC₆H₄)₂MePSe. Mp 158–160 °C (Found: C, 58.5; H, 5.85%. C₁₅H₁₇PSe requires C, 58.7; H, 5.57%).

(2-MeC₆H₄)₂^tBuPSe. Mp 164–166 °C (Found: C, 61.8; H, 6.81%. C₁₈H₂₃PSe requires C, 61.9; H, 6.65%).

11. Synthesis of (2-MeC₆H₄)₂MePCr(CO)₅ (6e). Dinitrogen was bubbled through a stirred degassed solution of Cr(CO)₆ (0.5 g, 2.19 mmol) and (2-MeC₆H₄)₂MeP (0.5 g, 2.19 mmol) in 1 : 1 THF–heptane (200 ml). The solution was irradiated for one hour (90 W mercury arc), filtered through Celite and evaporated to dryness. The crude product was purified by preparative TLC [silica, 1 : 9 CHCl₃–petroleum ether (bp 40–60 °C)] and recrystallised from petroleum ether (bp 60–80 °C) to give **6e** (0.6 g, 66%). **7e** was prepared in a similar manner.

(2-MeC₆H₄)₂MePCr(CO)₅. Mp 78–80 °C (Found: C, 57.4; H, 4.11%. C₂₀H₁₇CrO₅P requires C, 57.1; H, 4.08%).

(2-MeC₆H₄)₂^tBuPCr(CO)₅. Mp 130–32 °C (Found: C, 59.1; H, 4.99%. C₂₃H₂₃CrO₅P requires C, 59.7%; H, 5.02%).

Crystallographic studies

Data were collected on either an Enraf-Nonius CAD4f diffractometer (**3a**, **4a**, **5a**, **b** and **6b**, **c**, **e**) or an Enraf-Nonius Kappa CCDD detector (**7b**). Structures were solved by direct methods²⁶ and refined by full matrix least squares.²⁷ The structure of **7b** has already been deposited in the Cambridge Crystallographic Data Base (reference BAKTIR). See Table 4 for crystallographic data.

CCDC reference numbers 614969–6144975 and 6208454.

For crystallographic data in CIF or other electronic format see DOI: 10.1039/b610123b

Computational studies

All calculations were performed *in vacuo* using the Polak-Ribiere conjugate gradient algorithm for MM, semi-empirical and *ab initio* calculations. Investigations of conformational space for tri-arylphosphines combined several calculation approaches. Ground state conformations were sampled using the conformational search facility in ChemPlus. Conformations were generated by random rotation of named torsional angles employing a usage directed scheme which cycles through previously found conformations in order of increasing energy. Structures were optimised to a maximum of 750 or 1000 cycles depending on the structural complexity, with a convergence criterion of 0.075 kcal Å⁻¹ mol⁻¹. Post-optimisation, structures were rejected if they were in excess of 20 kcal mol⁻¹ higher in energy than the lowest energy accepted structure or if two consecutive structures had torsional angles within 5° or energies within 0.2 kcal mol⁻¹ of each other. Ring flip transition states were investigated by restraining ring torsional angles to ideal values (combinations of 0, 90 and 180°). High force constants (500 kcal mol⁻¹ degree⁻²) were applied and the geometry was optimised to a gradient of 0.075 kcal Å⁻¹ mol⁻¹ or a maximum of 750 cycles. The restraints were then removed and a single point energy calculated. For **1b**, all 26011 combinations of the three torsional angles ($\sum_1, \sum_3 = -180$ to $+180^\circ$, $\sum_2 = -180$ to 0° , 10° steps) were generated using a script of commands and geometries were optimised to a gradient of 0.1 kcal Å⁻¹ mol⁻¹ or a maximum of 1000 cycles, subject to restraints of 500 kcal mol⁻¹ degree⁻² on these angles. Restraints were then removed and single

Table 4 Crystallographic data

	3a	4a	5a	5b	6b	6c	6e	7b
Formula	C ₂₄ H ₂₇ P	C ₂₇ H ₃₃ P	C ₂₄ H ₂₇ P	C ₂₄ H ₂₇ OP	C ₁₅ H ₁₇ OP	C ₁₅ H ₁₇ PS	C ₂₀ H ₁₇ CrO ₅ P	C ₁₈ H ₂₃ OP
Habit	Monoclinic	Triclinic	Monoclinic	Monoclinic	Monoclinic	Monoclinic	Monoclinic	Orthorhombic
<i>a</i> /Å	10.737(2)	11.005(2)	7.4490(10)	14.398(2)	8.2401(9)	13.974(3)	10.763(1)	7.524(2)
<i>b</i> /Å	12.291(2)	12.990(3)	17.291(2)	8.274(2)	10.7830(9)	6.7730(10)	13.300(2)	13.097(3)
<i>c</i> /Å	15.286(2)	18.795(5)	15.649(2)	17.451(4)	15.5965(10)	15.790(4)	14.269(1)	16.665(3)
<i>a</i> /°		75.89(2)						
<i>β</i> /°	90.39(2)	88.14(2)	99.290(10)	101.973(16)	102.280(1)	111.380(1)	96.62(1)	90
<i>γ</i> /°		69.87(2)						
<i>λ</i> /Å	0.71069	0.71069	0.71069	0.71069	0.71069	0.71069	0.71069	0.71073
Space group	<i>P</i> ₂ ₁ / <i>n</i>	<i>P</i> ₁	<i>P</i> ₂ ₁ / <i>c</i>	<i>P</i> ₂ ₁ / <i>a</i>	<i>P</i> ₂ ₁ / <i>c</i>	<i>P</i> ₂ ₁ / <i>n</i>	<i>P</i> ₂ ₁ / <i>n</i>	<i>P</i> ₂ ₁ 2 ₁
<i>μ</i> /mm ⁻¹	0.139	0.121	0.141	0.145	0.185	0.323	0.669	0.162
<i>Z</i>	4	4	4	4	4	4	4	4
<i>θ</i> Range/°	2.13–24.98	2.12–21.97	2.36–24.98	2.39–31.99	2.31–27.96	2.44–29.96	2.10–29.97	1.98–27.38
Measured reflections	3874	6526	5567	5244	3572	4018	6371	10051
Independent reflections	3549	5976	3495	4853	3249	3742	5899	3602
<i>R</i>	0.0472	0.0517	0.0375	0.0444	0.0468	0.0618	0.0443	0.0420
<i>R</i> _w	0.1393	0.1568	0.1077	0.1189	0.1289	0.1811	0.1342	0.1093

point energies calculated. Due to the high symmetry of the energy surface, the remaining data points could be generated as a mirror image. Ring-substituent conformational space was explored using a script of driver calculations on the torsional angle $\tau = C_{\text{ring}} - C_{\text{ring}} - C_{\text{alkyl}} - C_{\text{alkyl}}$. For both ground and transition states, the selected torsional angle was driven in 10° increments from -180 to $+180^\circ$. The geometry was optimised to a gradient of $0.1 \text{ kcal } \text{Å}^{-1} \text{ mol}^{-1}$ or a maximum of 700 cycles using a large restraint ($500 \text{ kcal mol}^{-1} \text{ degree}^{-2}$) and after removal of restraints, a single point energy was calculated. If more than one ring bore substituents, driver calculations were performed successively on each substituent, allowing free adjustment of the remaining geometry. Using the same script, conformational preferences with respect to $\text{Cr}(\text{CO})_5$ orientation were explored.

In the case of diarylphosphines, all 1369 possible combinations of ring torsional angles (-180 to $+180^\circ$ on both rings, 10° steps) were generated and optimised to a gradient of $0.1 \text{ kcal } \text{Å}^{-1} \text{ mol}^{-1}$ or a maximum of 1000 cycles, applying a high torsional restraint ($500 \text{ kcal mol}^{-1} \text{ degree}^{-2}$). Removal of restraints was followed by a single point energy calculation. The barrier to rotation of the alkyl carbon–phosphorus bond was obtained similarly.

Acknowledgements

We wish to acknowledge the use of the EPSRC's Chemical Database Service at Daresbury.¹³ One of us (N.F.) also wishes to acknowledge financial support from Keele University and the Society for Chemical Industry for the award of a Messel Scholarship.

References

- For recent reviews of specific areas of catalysed asymmetric synthesis, see: (a) F. Speiser, P. Braunstein and W. Saussine, *Acc. Chem. Res.*, 2005, **38**, 784; (b) X. H. Cui and K. Burgess, *Chem. Rev.*, 2005, **105**, 3272; (c) S. Castillon, C. Claver and Y. Diaz, *Chem. Soc. Rev.*, 2005, **34**, 702; (d) A. M. Carroll, T. P. O'Sullivan and P. J. Guiry, *Adv. Synth. Catal.*, 2005, **347**, 609; (e) R. C. J. Atkinson, V. C. Gibson and N. J. Long, *Chem. Soc. Rev.*, 2004, **33**, 313; (f) T. P. Clark and C. R. Landis, *Tetrahedron: Asymmetry*, 2004, **15**, 2123; (g) K. V. L. Crepy and T. Imamoto, *Top. Curr. Chem.*, 2003, **229**, 1.
- For recent reviews, see: (a) D. Sinou, *Adv. Synth. Catal.*, 2002, **344**, 221; (b) N. Pinault and D. W. Bruce, *Coord. Chem. Rev.*, 2003, **241**, 1; (c) K. H. Shaughnessy and R. B. De Vasher, *Curr. Org. Chem.*, 2005, **9**, 585; (d) A. D. Phillips, L. Gonsalvi, A. Rornerosa, F. Vizza and M. Perruzzini, *Coord. Chem. Rev.*, 2004, **248**, 955.
- For recent reviews, see: (a) A. P. Dobbs and M. R. Kimberley, *J. Fluorine Chem.*, 2002, **118**, 3; (b) G. Pozzi and I. Shepperson, *Coord. Chem. Rev.*, 2003, **242**, 115.
- For recent reviews, see: (a) T. Welton, *Coord. Chem. Rev.*, 2004, **248**, 2459; (b) J. Dupont, R. F. de Souza and P. A. Z. Suarez, *Chem. Rev.*, 2002, **102**, 3667; (c) R. Sheldon, *Chem. Commun.*, 2001, 2399.
- For recent reviews, see: (a) W. Leitner, *Acc. Chem. Res.*, 2002, **35**, 746; (b) E. J. Beckman, *J. Supercrit. Fluids*, 2004, **28**, 121.
- For recent reviews, see: (a) D. E. Bergbreiter, *Top. Curr. Chem.*, 2004, **242**, 113; (b) C. Muller, M. G. Nijkamp and D. Vogt, *Eur. J. Inorg. Chem.*, 2005, 4011; (c) N. End and K. U. Schoning, *Top. Curr. Chem.*, 2004, **242**, 241.
- A. M. Gillespie, G. R. Morello and D. P. White, *Organometallics*, 2002, **21**, 3913 and references therein.
- (a) G. Ujaque and F. Maseras, *Struct. Bonding*, 2004, **112**, 117; (b) D. Balcells, G. Drudis-Sole, M. Besora, N. Dolker, G. Ujaque, F. Maseras and A. Lledos, *Faraday Discuss.*, 2003, **124**, 429.
- P. M. Todebush, G. Liang and J. P. Owen, *Chirality*, 2002, **13**, 220.
- (a) N. Fey, A. C. Tsipsis, S. E. Harris, J. N. Harvey, A. G. Orpen and R. A. Mansson, *Chem.–Eur. J.*, 2006, **12**, 291; (b) K. D. Cooney, T. R. Cundari, N. W. Hoffman, K. A. Pittard, M. D. Temple and Y. Zhao, *J. Am. Chem. Soc.*, 2003, **125**, 4318; (c) H. R. Bjorsvik, U. M. Hansen and R. Carlson, *Acta Chem. Scand.*, 1997, **51**, 733 and references therein.
- (a) C. P. Brock and J. A. Ibers, *Acta Crystallogr., Sect. B*, 1973, **29**, 2426; (b) D. C. Levendis and I. Bernal, *Struct. Chem.*, 1997, **8**, 263.
- D. A. Fletcher, R. F. McMeeking and D. Parkin, *J. Chem. Inf. Comput. Sci.*, 1996, **36**, 746.
- J. Bruckmann and C. Krueger, *J. Organomet. Chem.*, 1997, **536**, 465–537.
- K. A. Jensen and P. H. Nielsen, *Acta Chem. Scand.*, 1963, **17**, 1875.
- (a) M. L. Caffery and T. L. Brown, *Inorg. Chem.*, 1991, **30**, 3907; (b) K. J. Lee and T. L. Brown, *Inorg. Chem.*, 1992, **31**, 289.
- J. A. S. Howell, P. C. Yates, M. G. Palin, P. McArdle, D. Cunningham, Z. Goldschmidt, H. E. Gottlieb and D. Hezroni-Langerman, *J. Chem. Soc., Dalton Trans.*, 1993, 2775.
- (a) A. G. Hopfinger and R. A. Pearlstein, *J. Comput. Chem.*, 1984, **5**, 486; (b) P. Ugliengo, J. Ahmed, D. Viterbo and M. Ceruti, *Gazz. Chim. Ital.*, 1989, **119**, 493.
- HyperChem 5.11*, Hypercube Inc., Gainesville, FL, 2002.
- 2-MeC₆H₄ series: (a) J. A. S. Howell, M. G. Palin, P. C. Yates, P. McArdle, D. Cunningham, Z. Goldschmidt, H. E. Gottlieb and D. Hezroni-Langerman, *J. Chem. Soc., Perkin Trans. 2*, 1992, 1769; (b) T. S. Cameron and B. Dahlen, *J. Chem. Soc., Perkin Trans. 2*, 1975, 1737.
- 2-CF₃C₆H₄ series: J. A. S. Howell, N. Fey, J. D. Lovatt, P. C. Yates, P. McArdle, D. Cunningham, E. Sadeh, H. E. Gottlieb, Z. Goldschmidt, M. B. Hursthouse and M. E. Light, *J. Chem. Soc., Dalton Trans.*, 1999, 3015.
- (a) K. Mislow, *Chemtracts: Org. Chem.*, 1989, **2**, 151; (b) K. Mislow, D. Gust, R. J. Finocchiaro and R. J. Boettcher, *Top. Curr. Chem.*, 1974, **47**, 1.
- See references 23, 24 in reference 20.
- I. O. Sutherland, *Annu. Rep. NMR Spectrosc.*, 1971, **4**, 80.
- For an alternative synthesis, see: G. M. Whitesides, M. Eisenhut and W. M. Bunting, *J. Am. Chem. Soc.*, 1974, **96**, 5368.
- B. Åkermark and A. Ljungqvist, *J. Organomet. Chem.*, 1978, **149**, 97.
- G. M. Sheldrick, *SHELXS-97*, *Acta Crystallogr., Sect. A*, 1990, **46**, 467.
- G. M. Sheldrick, *SHELXL97*, University of Göttingen, Germany, 1997.